

# Abrasively modified electrodes: mathematical modelling and numerical simulation of electrochemical dissolution/growth processes under cyclic voltammetric conditions

Electrochemically reversible and irreversible processes at well-separated particles

François G. Chevallier · Alex Goodwin ·  
Craig E. Banks · Li Jiang · Timothy G. J. Jones ·  
Richard G. Compton

Received: 22 March 2006 / Revised: 29 March 2006 / Accepted: 5 April 2006 / Published online: 8 June 2006  
© Springer-Verlag 2006

**Abstract** An approximate mathematical model for electrochemical dissolution/growth processes of diffusionally independent and well-separated particles randomly dispersed on an inert conducting electrode surface is presented and solved using numerical simulation. The model, mimicking abrasively modified electrodes where particles of electroactive voltammograms solid are immobilised on an electrode surface, provides clear insights into the effects of different parameters on the voltammetric response of such systems and permits the exploration of the competition taking place between mass transport and surface processes. The mathematical model is then compared with experimental data obtained with basal plane pyrolytic graphite electrode abrasively modified with solid particles of perinaphthenone and studied in aqueous solution.

**Keywords** Partially electrochemical dissolution ·  
Cyclic voltammetry · Numerical simulation ·  
Abrasively modified electrodes

---

Dedicated to Professor Dr. Alan M. Bond on the occasion of his 60th birthday.

---

F. G. Chevallier · A. Goodwin · C. E. Banks · R. G. Compton (✉)  
Physical and Theoretical Chemistry Laboratory,  
Oxford University,  
South Parks Road,  
Oxford OX1 3QZ, UK  
e-mail: richard.compton@chemistry.ox.ac.uk

L. Jiang · T. G. Jones  
Schlumberger Cambridge Research, High Cross,  
Madingley Road,  
Cambridge CB3 0EL, UK

## Introduction

The abrasive deposition of solid particles on a soft working electrode [1–3] has been increasingly used to explore the voltammetry of solid materials and also as a mean of qualitative analysis after the pioneering work of Scholz [1]. This method is attractive because of its facile implementation and its wide and generic range of application [2].

Abrasively modified electrodes are often composed of different solid phases, and are often characterised by electrochemical stripping analysis [3]: electrochemically induced dissolution leads to the potential-driven conversion of a solid species to soluble products and the resulting voltammograms are used to generate thermodynamic and, in principle, kinetic data.

There have been a number of publications in the literature dealing with the mathematical treatment of such reactions [4–12]. However, a significant proportion of this work either uses a treatment based on some simplifying assumptions or does not provide a rigorous quantitative treatment of the results. Simplified analytical treatments have been performed by various authors. Simplified models for irreversible dissolution reactions have been presented, for example, in a series of publications concerning iron oxides by Mouhandess et al. [6, 7, 12]. In this case, the authors assumed that the voltammetric response was essentially surface controlled and the model did not include any mass transport contribution. Others authors such as Brainina and Vydrevich [4] or Grygar [5] have introduced models based on a thin-layer approach or involving one-dimensional diffusion; this latter approach assumes effectively that the electrode surface is uniform and homogeneous. It is clear that such models have only limited application and should be used with care.

In this paper, we use our previous experience with spatially heterogeneous electrodes to develop a more

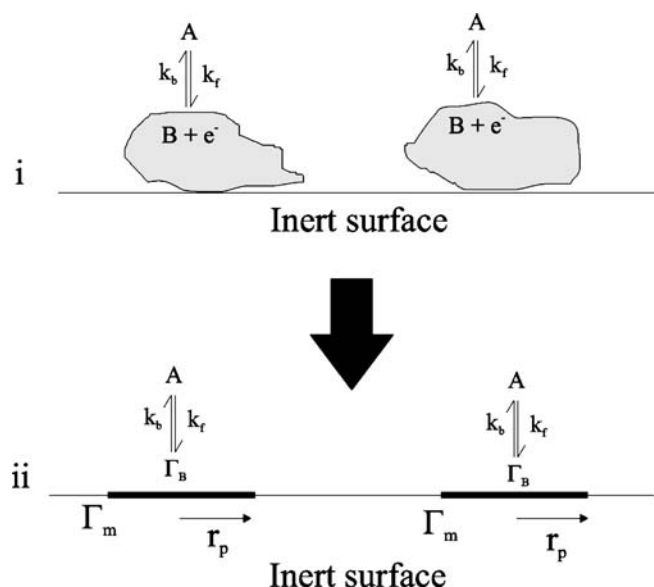


**Fig. 1** Schematic representation of the dissolution/growth process (a) real physical system and (b) simplified physical system

general model for electrochemically reversible electro-dissolution reactions. Our previous work with partially blocked electrodes clearly showed that heterogeneous surfaces had non-negligible effects on the mass transport behaviour, so that a simplified mathematical model was not sufficient to fully describe the electrochemical behaviour of these kind of modified electrodes [13–18]. Our approach is based on the diffusion domain approximation introduced in previous publications [13–18]. A computer program for numerical simulation of the corresponding mathematical model is constructed allowing for the investigation of the voltammetric response of such systems; in particular, we emphasise the interplay existing between mass transport and the surface kinetics. Especially noteworthy is the strong asymmetry with respect to the potential-driven dissolution and solid formation processes seen in the different parts of the cyclic voltammetric response. We report experiments confirming the excellent agreement between theory and practice in respect of the voltammetry of abrasively immobilised perinaphthenone (C<sub>13</sub>H<sub>8</sub>O).

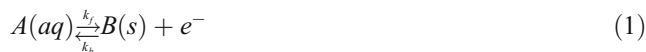
### Mathematical model and numerical simulation

We consider an electrochemically inert surface of area  $A_s$  covered with  $N$  well-separated particles of material  $B$  of identical volume. The reaction of interest is the electrochemical dissolution/growth of the  $B$  particles (see Fig. 1). For the sake of simplicity, we will ignore the volume of the particles, instead approximating them by flat disks of radius  $r_p$  characterised by an initial surface concentration  $\Gamma_m$  and a time/position dependent concentration  $\Gamma_B$  (Fig. 1). The

dissolution/growth reaction is then modelled by an adsorption/desorption reaction of Langmuirian type [19, 20]. These hypotheses allow us to simplify the problem sufficiently, so that it is mathematically tractable, whilst remaining realistic enough for the analysis to be meaningful. The particles are assumed to be randomly distributed over the electrode surface; therefore, the global electrochemical response of the surface is modelled using the diffusion domain approximation, which has been extensively introduced in previous publications [17, 18] and will therefore not be described in this study. The electrochemical response of the system is therefore given by the sum of the response of individual diffusion domains. This generic approach has already been used for partially blocked and porous electrodes and has been shown to be computationally very efficient whilst retaining physical accuracy [13–18]. Finally, we will constrain our analysis to the case of well-separated particles; in other words, for all time, the particles are sufficiently separated not to interfere with each other's diffusional domain.

### Mathematical model for a single diffusion domain

We consider a redox couple at the particle surface with Butler–Volmer-like kinetics:



where  $A$  is an ion whilst  $B$  is a solid.  $k_f$  and  $k_b$  are the forward and backward rate constants defined by:

$$k_b = k_0[A]^0 \exp\left(\frac{(1-\alpha)F}{RT}(E - E^0)\right) \quad (2)$$

where  $k_0$  is the surface process rate constants for the  $A/B$  couple with units  $\text{cm}\cdot\text{s}^{-1}$ ,  $\alpha$  is the transfer coefficient and  $E^0$  is the formal potential and  $[A]^0$  is the standard concentration equal to  $1 \times 10^{-3} \text{ mol}\cdot\text{cm}^{-3}$ .

The expression for  $k_f$  and  $k_b$  reflects the differing standard states adopted by thermodynamics for solutes and solid and can be checked using the equilibrium properties of the physical system. When equilibrium is reached, the following relationship holds:

$$k_f(\Gamma_m - \Gamma_B)[A]_{\text{surf}} = k_b\Gamma_B \tag{3}$$

Simple algebraic manipulation leads to:

$$e^{\frac{F}{RT}(E-E^0)} = \frac{(1-\theta)[A]_{\text{surf}}}{\theta[A]^0} \tag{4}$$

where  $\theta = \Gamma_B/\Gamma_m$ , this can be rewritten as:

$$E = E^0 + \frac{RT}{F} \ln \left( \frac{[A]}{[A]^0} \right) \tag{5}$$

Which is the Nernst equation corresponding to the process presented in Fig. 1b. The mass transport of species  $A$  to the surface in the cylindrical coordinate system, as well as the evolution of the surface concentration  $\Gamma_B$  are described by the following set of equations:

$$\Gamma_m \frac{\partial \Gamma_B}{\partial t} = k_f(\Gamma_m - \Gamma_B)[A]_{\text{surf}} - k_b\Gamma_B \tag{6}$$

where  $D_A$  is the diffusion coefficient of species  $A$  and the other parameters have been defined previously or have their usual meaning. Before the electrochemical experiment is started, only species  $B$  is present in solid state. Therefore, the initial conditions ( $t=0$ ) for the species taking part in the reaction are:

$$\begin{aligned} [A] &= 0 & \text{for } 0 \leq r \leq r_0 & \text{ and } 0 \leq z < \infty \\ \Gamma_B &= 0 & \text{for } 0 \leq r < r_p & \text{ and } z = 0 \end{aligned} \tag{7}$$

The geometrical shape of the simulation space implies a zero concentration of  $A$  at the semi-infinite boundary as well as a non-flux boundary conditions on the symmetry axis, the diffusion domain wall and on the electrode surface, this is translated mathematically as:

$$\begin{aligned} [A] &= 0 & \text{for } 0 \leq r \leq r_0 & \text{ and } z \rightarrow \infty \\ \frac{\partial [A]}{\partial r} &= 0 & \text{for } r = 0 & \text{ and } 0 \leq z < \infty \\ \frac{\partial [A]}{\partial r} &= 0 & \text{for } r = r_0 & \text{ and } 0 \leq z < \infty \\ \frac{\partial [A]}{\partial z} &= 0 & \text{for } r_p \leq r \leq r_0 & \text{ and } z = 0 \end{aligned} \tag{8}$$

At the particle surface, we have the following condition:

$$\begin{aligned} D_A \frac{\partial [A]}{\partial z} &= \frac{\partial \Gamma_B}{\partial t} = k_f(\Gamma_m - \Gamma_B)[A]_{\text{surf}} - k_b\Gamma_B & \text{for} \\ r &= 0 \text{ and } 0 \leq z < \infty \end{aligned} \tag{9}$$

The boundary conditions presented in this study are relatively realistic with respect to the simulation of anodic stripping voltammetry where the particles are conductive. For the case of abrasively modified electrodes, this may be less so but it is recognised that such electrolysis proceeds at the three phase boundary formed by the solid, the substrate electrode, and the electrolyte solution [21, 22]; in this case, at the perimeter of the solid in contact with the electrode. In our model, this is partially mimicked by the high current densities observed at the circumference of the disks under mass transport control. Moreover, because under these conditions the disk dissolution will be non-uniform with more material dissolving most rapidly at the disk edges, the model describes the shrinkage of the particle as dissolution proceeds. This is described through the radial dependence of  $\Gamma_B$ . The value of  $\Gamma_B$  is initially uniform and equal to  $\Gamma_m$  but becomes progressively more depleted at the disk edges during dissolution. In this way, the model captures, in an approximate way, the three-phase boundary. Therefore, for each diffusion domain the current flow can be calculated using the following expression:

$$I = -2\pi F \int_0^{r_p} \frac{\partial \Gamma_B}{\partial t} r dr \tag{10}$$

Because the surface concentration of the particle is not only a function of time but also a function of position, the interpretation of the results can be simplified by introducing an average surface concentration defined as:

$$\bar{\Gamma}_B = \frac{2}{r_d^2} \int_0^{r_p} \Gamma_B r dr \tag{11}$$

### Computation

A fully implicit discretization scheme [23] combined with Newton’s method [23] and a modified version of the Thomas algorithm [24] was used to solve the system of partial differential equations. The simulation space was covered with an expanding grid similar to the one presented in previous publications [13–16] and which will therefore not be described in this study. The simulation program was tested for both spatial and temporal convergence to ensure that the solution satisfies the accuracy requirement for the quantity of interest [17, 18] (less than 1% variation from the asymptotic peak current value for all scan rates considered). All the programs for the simulations were written in Delphi 7 and executed on a PC with Pentium 4 2.5 GHz processor

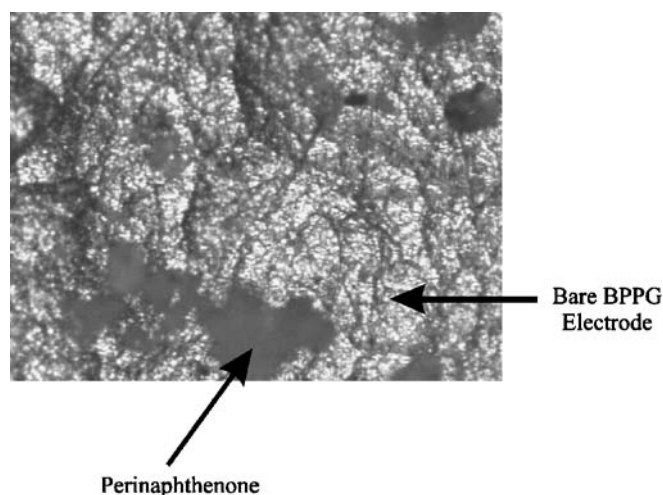


**Fig. 2** An optical image of a bppg electrode abrasively modified with perinaphthenone. Image size 500×540  $\mu\text{m}$

and 1 GB of RAM. The convergence and accuracy of the simulation program were tested in the same way as described in previous publications [17, 18].

## Experimental

### Chemical reagents and instrumentation

All chemicals were of analytical grade and used as received without any further purification. These were perinaphthenone (>97%, Aldrich), boric acid (Aldrich, >99.5%) and NaOH (Acros, Analar grade). Solutions were prepared with deionised water of resistivity not less than 18.2  $\text{M}\Omega\cdot\text{cm}$  (Millipore water systems, UK). Voltammetric measurements were carried out using a  $\mu$ -Autolab II potentiostat (Eco-Chemie, The Netherlands) with a three-electrode configuration. Basal plane pyrolytic graphite (bppg, Le Carbone, Sussex, UK) was used as the working electrode (electrochemically inert under the experimental conditions used).

The bppg electrode was fabricated from a sheet of pyrolytic graphite which was machined into 4.9 mm diameter disks. These disks were oriented with the face parallel with the edge plane, or basal plane as required. The counter electrode was a bright platinum wire, with a saturated calomel electrode completing the circuit. The basal plane pyrolytic graphite electrode was prepared by

renewing the electrode surface with cellotape. This procedure involves polishing the bppg electrode surface on Carborundum paper (P100 grade) and then pressing cellotape on the cleaned bppg surface, which is removed along with attached graphite layers. This is then repeated several times.

The electrode was then cleaned in water and acetone to remove any adhesive [25]. The bppg electrode was abrasively modified with perinaphthenone by gently rubbing a freshly prepared bppg electrode on a piece of fine quality filter paper along with the perinaphthenone (see Fig. 2). All experiments were typically conducted at  $293\pm 2$  K. Before commencing experiments, nitrogen (BOC, Surrey, UK) was used for deaeration of solutions.

## Results and discussion

### Theoretical results

The electrochemical behaviour of dissolution/growth processes is essentially dependent on the interactions of two phenomena: the mass transport in the solution and the surface process leading to the formation of the solid material. The way these two processes interact dictates the shape of the voltammetric response and in particular the magnitude of the forward and backward peaks ( $I_{\text{pf}}$  and  $I_{\text{pb}}$ , respectively).

A good approach to gain a better understanding of this system is to study the variation of the peak magnitude as a function of different parameters. From “[Mathematical model and numerical simulation](#)” section, we can easily see that different parameters affect the peak currents; however, the influence of certain parameters such as  $D_A$  and  $\Gamma_m$  is easy to assess. Consequently, we will focus our study on the influence of other parameters such as the

**Table 1** Scan rate and desorption rate constant values used for simulation

Parameter	Values
Scan rate $v/V$	From 0.1 to 5
Surface rate constant $k_0/\text{cm}\cdot\text{s}^{-1}$	From $1\times 10^{-8}$ to 1

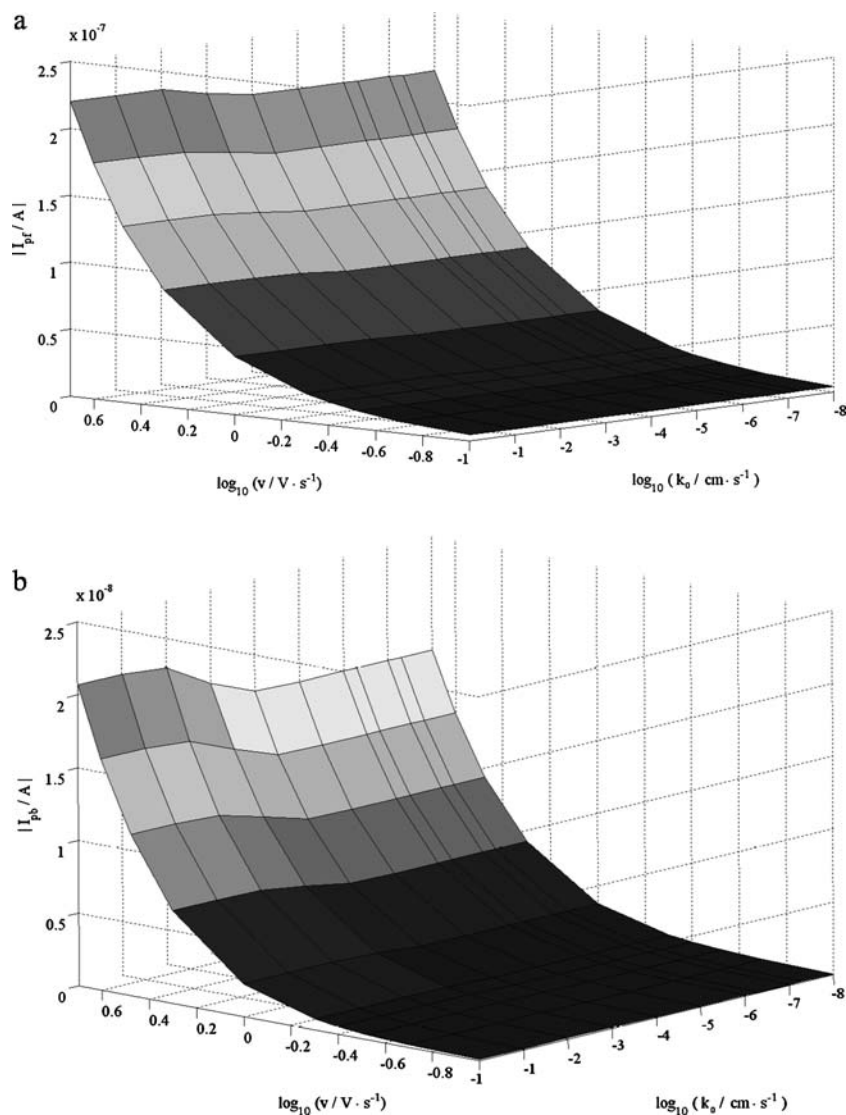


**Fig. 3** Variation of (a)  $|I_{pf}|$  and (b)  $|I_{pb}|$  as a function of  $\nu$  and  $k_0$  for an independent diffusion domain. The parameters used for simulation are as follows:  $[A]^0=1 \times 10^{-3} \text{ mol}\cdot\text{cm}^{-3}$ ,  $r_p=1 \times 10^{-3} \text{ cm}$ ,

$D_A=1 \times 10^{-6} \text{ cm}^2\cdot\text{s}^{-1}$ ,  $\Gamma_m=1 \times 10^{-6} \text{ mol}\cdot\text{cm}^2$ ,  $\alpha=0.5$ ,  $E_{\text{start}}=-1 \text{ V}$ ,  $E_{\text{reverse}}=1 \text{ V}$ ,  $E^0=0 \text{ V}$ ,  $7\sqrt{\frac{2D_A(E_{\text{reverse}}-E_{\text{start}})}{\nu}} \text{ cm}$  and the values of  $\nu$  and  $k_0$  are given in Table 1

surface process rate constant  $k_0$  and the voltage scan rate  $\nu$  (the values used for simulation are shown in Table 1).

Figure 3 presents the evolution of the forward and backward peak currents ( $I_{pf}$  and  $I_{pb}$ , respectively) as a function of scan rate and desorption rate constant (the simulation parameters are given in the figure legend). As it can be seen from the picture, both peak currents' intensities increase as the scan rate increases. This is expected as the scan rate directly affects the speed at which  $B$  dissolves and an increasing value of  $\nu$  also leads to a more constrained diffusion layer, making it easier for  $A$  to reach the electrode surface and, therefore, increasing the value of  $I_{pb}$ .

The influence of  $k_0$  on the voltammetric response is less obvious.  $k_0$  is not expected to dramatically affect the peak

current value but should shift the observed peak potential. This is clearly visible from Fig. 3 as, for a wide range of  $k_0$  values, no significant variations of  $I_{pf}$  and  $I_{pb}$  are visible. However, for small values of  $k_0$  and relatively high scan rate values, the electrochemical system exhibits a different behaviour leading to a decrease of both peak currents' magnitude. The phenomenon observed is comparable to the transition between quasi-reversible and irreversible electrode kinetics characteristic of conventional electrochemical systems.

One of the main features of the system under investigation is the dramatic difference in magnitude observed between the forward and the backward peak values. This strong asymmetry contrasts with what is observed in



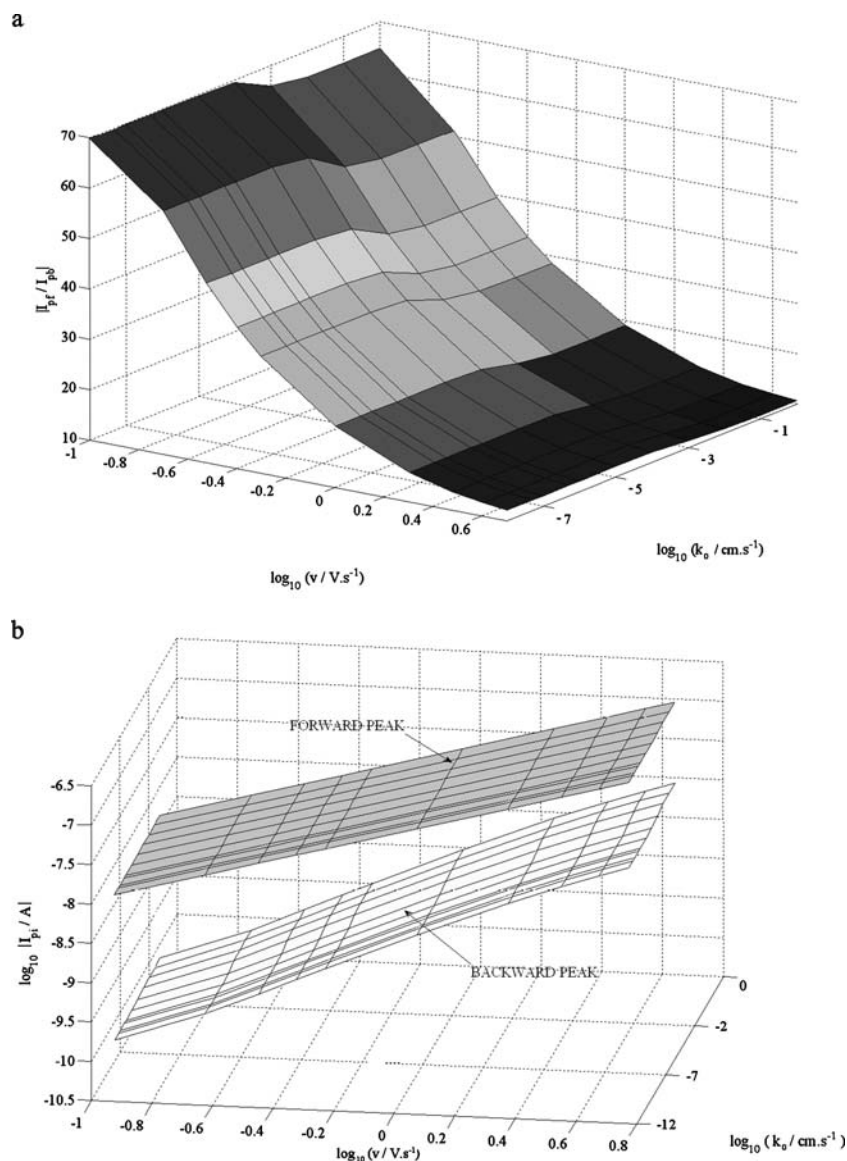


**Fig. 4** Variation of **a**  $|I_{pf}/I_{pb}|$  and **b**  $|I_{pi}|$  as a function of  $\nu$  and  $k_0$  for an independent diffusion domain. The parameters used for simulation are as follows:  $[A]^0=1 \times 10^{-3} \text{ mol}\cdot\text{cm}^{-3}$ ,  $r_p=1 \times 10^{-3} \text{ cm}$ ,

$D_A=1 \times 10^{-6} \text{ cm}^2\cdot\text{s}^{-1}$ ,  $\Gamma_m=1 \times 10^{-6} \text{ mol}\cdot\text{cm}^{-2}$ ,  $\alpha=0.5$ ,  $E_{\text{start}}=-1 \text{ V}$ ,  $E_{\text{reverse}}=1 \text{ V}$ ,  $E^0=0 \text{ V}$ ,  $7\sqrt{\frac{2D_A(E_{\text{reverse}}-E_{\text{start}})}{\nu}} \text{ cm}$  and the values of  $\nu$  and  $k_0$  are given in Table 1

aqueous phase electrochemistry. As a consequence, understanding of this system can be greatly improved by studying the variation of the peak current ratio defined as  $I_{pf}/I_{pb}$ . The results are shown in Fig. 4a; the figure also presents the variation of the natural logarithms of both peak currents to emphasise the differences existing between them (Fig. 4b). Figure 4a clearly shows the kinetic transition mentioned above; it can also be seen that the value of the ratio increases as the scan rate decreases. This can be understood with the help of Fig. 4b. As the scan rate decreases, the time scale of the experiment increases and so does the diffusion layer thickness. These conditions have a conventional effect on the forward peak current, e.g. the

value of  $I_{pf}$  decreases. However, when the reverse scan begins, the surface process is in direct competition with the diffusion process of  $A$  in the bulk solution and if the speed of the surface process is not fast enough, then  $A$  tends to diffuse into the bulk solution instead of diffusing to the electrode surface. Hence, the intensity of  $I_{pb}$  decreases and the value of  $I_{pf}/I_{pb}$  increases.

#### Experiments and comparison with theory

A freshly prepared basal plane pyrolytic graphite electrode was abrasively modified with perinaphthenone and immersed into a pH 10 boric buffer solution with the cyclic

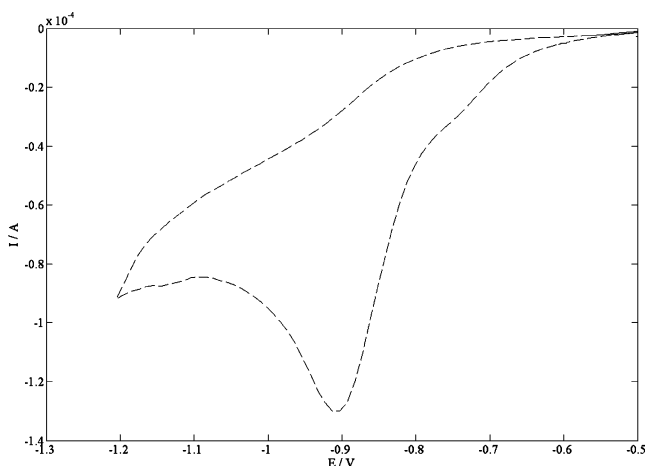


**Fig. 5** Cyclic voltammetric response of a perinaphthenone abrasively modified basal plane pyrolytic graphite electrode in a pH 10 boric buffer solution at a scan rate of  $0.1 \text{ V}\cdot\text{s}^{-1}$

voltammetric response explored. Figure 5 shows the voltammetric profile where the chemically irreversible reduction of perinaphthenone occurs after the scheme presented in Fig. 6. This is identical to that reported by Wain et al. [26] who studied the electrochemical reduction of perinaphthenone in both aqueous and non-aqueous solutions. At pH values greater than 9, the cathodic reduction product of perinaphthenone is the radical anion [26]. At conventional scan rates, irreversible voltammetry is observed [26] as shown in Fig. 5. Next, a freshly prepared basal plane pyrolytic graphite electrode was modified with perinaphthenone and immersed into a pH 10 boric buffer solution with the cyclic voltammetric response explored over a range of scan rate values ( $3$  to  $14.5 \text{ V}\cdot\text{s}^{-1}$ ).

Figure 7 presents the variations of  $I_{\text{pf}}/I_{\text{pb}}$  for both experimental results and numerical simulation for a wide range of scan rates. The observed scatter in the experimental data is due to the fact that for each scan rate the electrode is newly prepared and modified. Simulation of the variation of  $I_{\text{pf}}/I_{\text{pb}}$ , rather than individual peak currents was chosen, as this ratio is a good indicator of the interactions between mass transport and surface kinetic. The values of the simulation parameters were obtained using experimental data as described in the legend of Fig. 7. As it can be seen from Fig. 7, theory and experiment are in good agreement; thus, confirming that the model presented in “Mathematical model and numerical simulation” section is realistic.

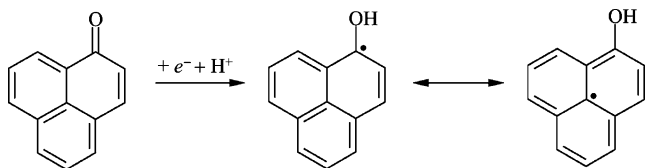


**Fig. 6** Scheme of the reduction of perinaphthenone

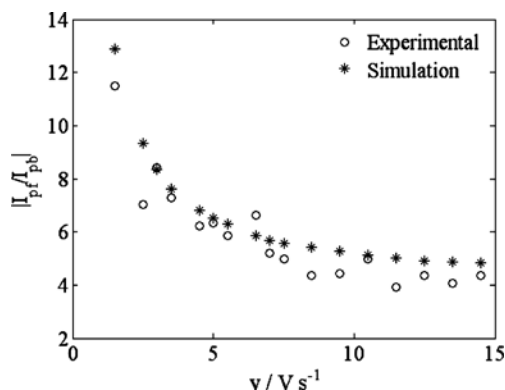


**Fig. 7** Comparison of experimental data with simulation for the evolution of  $|I_{\text{pf}}/I_{\text{pb}}|$  with scan rate. Experimental data corresponds to perinaphthenone rubbed onto a basal plane electrode of surface area  $A_s=0.196 \text{ cm}^2$ ; the number of particles present on the electrode surface,  $N$ , was visually estimated to be equal to 1,000 using optical microscopy and the corresponding mass of perinaphthenone was calculated using voltammetric data. The parameters used for simulation are as follows:  $[A]^0=1\times 10^{-3} \text{ mol}\cdot\text{cm}^{-3}$ ,  $r_p=3.9\times 10^{-4} \text{ cm}$ ,  $D_A=6\times 10^{-6} \text{ cm}^2\cdot\text{s}^{-1}$ ,  $\Gamma_m=2.6\times 10^{-4} \text{ mol}\cdot\text{cm}^2$ ,  $\alpha=0.5$ ,  $E_{\text{start}}=-1.2 \text{ V}$ ,  $E_{\text{reverse}}=0.5 \text{ V}$ ,  $E^0=0 \text{ V}$ ,  $r_0=8\times 10^{-3} \text{ cm}$  and  $k_0=1\times 10^{-1} \text{ cm}\cdot\text{s}^{-1}$

### Conclusion

This work allowed for qualitative and quantitative studies of electrochemical dissolution/growth processes of diffusionally independent particles randomly distributed on an electrochemically inert surface. We have highlighted the influence of parameters such as the desorption rate constant and the scan rate on the global voltammetric response of such systems as well as the competition taking place between mass transport and the surface process.

The mathematical model presented in this publication has been validated through comparison with experimental data obtained with a basal plane pyrolytic graphite electrode abrasively modified with perinaphthenone. The model presented in this study can be useful for qualitative and quantitative characterization of the relative speed of the different processes involved in such electrochemical systems. In future work, we intend to use and to extend the mathematical modelling presented in this study to the investigation of anodic stripping voltammetry.

**Acknowledgement** We thank Schlumberger Cambridge Research for a studentship for FGC.

### References

- Scholz F, Schroder U, Gulaboski R (2005) Electrochemistry of immobilized particles and droplets. Springer, Berlin Heidelberg New York

2. Grygar T, Marken F, Schroder U, Scholz F (2002) Collection of Czechoslovak chemical communications 67(2):163
3. Brainina K, Neyman E (1993) Electroanalytical stripping methods. Wiley, New York
4. Brainina K, Vydrevich MJ (1981) *J Electroanal Chem* 121:1
5. Grygar TJ (1998) *J Solid State Electrochem* 2:127
6. Mouhandess M, Chassagneux F, Vittori O (1982) *J Electroanal Chem* 131:367
7. Mouhandess M, Chassagneux F, Durand B, Sharara Z, Vittori O (1985) *J Mater Sci* 20:3289
8. Brainina K, Lesunova R (1974) *Zh Anal Khim* 29:117
9. Manzoli A, Santos MC, Bulhoes LOS (2006) *Surf Coat Technol* 200(9):2990
10. Nazarov BF, Stromberg AG (2005) *Russ J Electrochem* 41(1):49
11. Nechiporuk VV, Berladin IV, Slipenyuk TS (2005) *Visnik Kharkiv-s'kogo Natsional'nogo Universitetu im. V.N. Karazina* 648:43
12. Mouhandess M, Chassagneux F, Vittori O, Accary A, Reeves RJ (1984) *J Electroanal Chem* 181:93
13. Brookes BA, Davies TJ, Fisher AC, Evans RG, Wilkins SJ, Yunus K, Wadhawan JD, Compton RG (2003) *J Phys Chem B* 107(7):1616
14. Davies TJ, Brookes BA, Fisher AC, Yunus K, Wilkins SJ, Greene PR, Wadhawan JD, Compton RG (2003) *J Phys Chem B* 107(26):6431
15. Davies TJ, Brookes BA, Compton RG (2004) *J Electroanal Chem* 566(1):193
16. Davies TJ, Banks CE, Compton RG (2005) *J Solid State Electrochem* 9(12):797
17. Chevallier FG, Davies TJ, Klymenko OV, Jiang L, Jones TGJ, Compton RG (2005) *J Electroanal Chem* 577(2):211
18. Chevallier FG, Davies TJ, Klymenko OV, Jiang L, Jones TGJ, Compton RG (2005) *J Electroanal Chem* 580(2):265
19. Harman AR, Baranski AS (1991) *Anal Chem* 63:1158
20. Szulborska A, Baranski AS (1994) *J Electroanal Chem* 377:269
21. Scholz F, Lange B (1992) *Trends Anal Chem* 11:359
22. Scholz F, Meyer B (1994) *Chem Soc Rev* 341
23. Eriksson K, Estep D, Hansbo P, Johnson C (1996) *Computational differential equations*. Cambridge University Press, Cambridge, UK
24. Svir I, Klymenko OV, Compton RG (2001) *Radiotekhnika* 118:92
25. Moore RR, Banks CE, Compton RG (2004) *Anal Chem* 76:2677
26. Wain AJ, Drouin L, Compton RG (2006) *J Electroanal Chem* 589(1):128